

## Optimizing the ITER Heating and Current Drive Mix

F. Wagner 1), M. Henderson 2), B. Beaumont 2), A. Becoulet 3), D. Boilson 2), R. Budny 4), D. Campbell 2), C. Darbos 2), V. Erckmann 1), D. Farina 5), G. Giruzzi 3), R. Hemsworth 2), Y. Kamada 6), A. Kaye 7), F. Kazarain 2), F. Koechl 8), K. Lackner 1), P. Lamalle 2), N. Marushchenko 1), M. Murakami 9), T. Oikawa 10), V. Parail 11), J.M. Park 9), G. Ramponi 5), O. Sauter 12), J. Snipes 2), D. Stork 11), A. Tanga 2), P.R. Thomas 13), Q.M. Tran 12), D. Ward 11), H. Zohm 1), C. Zucca 12)

- 1) Max-Planck Institut für Plasmaphysik, EURATOM Association, Garching/Greifswald, Germany.
- 2) ITER Organization, Route de Vinon sur Verdon, F-13115 St Paul lez Durance, France.
- 3) CEA, IRFM, F-13108 Saint-Paul-lez-Durance, France.
- 4) Princeton Plasma Physics Laboratory, Princeton, New Jersey 08543.
- 5) Istituto di Fisica del Plasma, EURATOM- ENEA-CNR Association, 20125 Milano, Italy.
- 6) Japan Atomic Energy Research Institute, Naka Fusion Research Establishment, Naka-machi, Naka-gun, Ibaraki-ken 311-01, Japan.
- 7) Consultant, Oxford OX12 7HA, UK.
- 8) Association EURATOM-ÖAW/ATI, Atominstitut, TU Wien, Austria.
- 9) Oak Ridge National Laboratory, Oak Ridge, Tennessee 37831.
- 10) EFDA Close Support Unit, Boltzmannstrasse 2, D-85748 Garching, Germany.
- 11) Euratom/CCFE Fusion Association, Culham Science Centre, Abingdon, OX14 3DB, UK.
- 12) Centre de Recherches en Physique des Plasmas, Association Euratom-Confédération Suisse, EPFL, 1015 Lausanne, Switzerland.
- 13) Fusion for Energy, Joint Undertaking, 08019 Barcelona, Spain.

E-mail contact of main author: fritz.wagner@ipp.mpg.de

**Abstract.** ITER will be heated in the first stage by 20/33/20 MW ECH, NBI and ICH (reference heating mix). The balance between the three heating systems has been evaluated considering two scenarios: an ELMy H-mode and a quasi steady-state non-inductive mode of operation. The analysis included modeling of the current drive efficiency of each heating system. For the EC system, two momentum conserving codes were used (CQL-3D and TRAVIS), which showed consistency. Modeling of the NBCD efficiency,  $\gamma_{\text{NBCD}}$ , was done with OFMC and NUBEAM. Both ECH and NBI show similarly high  $\gamma$ -values in the core.  $\gamma_{\text{NBCD}}$  stays fairly constant with radius qualifying NBCD for global CD;  $\gamma_{\text{ECCD}}$  drops, however, sharply toward the edge. The following observations were made: With sufficient edge stability,  $Q = 10$  is possible with NBI, ICH or ECH. ICH heats selectively the ions and increases fusion gain by  $\Delta Q \sim 1$ . The  $Q = 5$ , quasi-steady-state condition requires discharges with  $f_{\text{bs}} > 50\%$  and strong current drive. ECCD deposited off-axis can initiate reversed shear scenarios but not effectively drive the current. This can only be achieved by NBI. With beams, inductive discharges with  $f_{\text{ni}} > 80\%$  and  $Q \sim 5$  can be maintained for 3000 s. The analysis demonstrates that the chosen power mix exploits the strengths of each heating system and provides the necessary actuators for advanced scenarios to respond in a flexible way. A summary of this analysis is provided along with a brief review of the technical challenges still facing each heating system prior to procurement and their installation on ITER.

### 1 Introduction

The ITER project has two clear goals: the demonstration of the fusion gain  $Q = P_{\text{fus}}/P_{\text{aux}} > 10$  for a pulse length of 300 – 500 s in inductive ELMy H-mode (referred to as Scenario-2) and secondly, to reach  $Q = 5$  under quasi-steady-state non-inductive conditions (referred to as Scenario-4). Success in achieving these goals depends on the characteristics of external heating and current drive systems, to effectively heat the plasma, drive the plasma current non-inductively with a high efficiency  $\gamma = I_{\text{CD}} n_e R / P_{\text{CD}}$ , and produce plasma states with sufficient confinement, well controlled MHD activity and high bootstrap current fractions. The heating power must be above the DT H-

mode power threshold, which is estimated to be 70 MW for Scenario-2 ( $\langle n_e \rangle = 1 \cdot 10^{20} \text{ m}^{-3}$ ) and 50 MW for the lower-density Scenario-4. The heating power of ITER in the first stage is 73 MW of absorbed power in the mix of 20/33/20 MW ECH, NBI and ICH. In the L-mode prior to the transition  $P_\alpha \approx 40$  MW and ITER will be limited to  $Q \approx 2-3$  in Scenario-2 if the H-mode is not achieved. The frequencies of ECH and ICH are 170 GHz and 40-55 MHz and are matched to the respective resonance conditions of the considered heating scenarios. The beam energy is targeted at 1 MeV for plasma core accessibility and for high current drive efficiency. All three systems heat the plasma effectively under proper conditions. An evaluation of the ITER heating and current drive mix has been performed [1] with the aim to ensure an optimum balance between the powers of the three initial heating systems. This paper attempts to summarize that study and to report on the technical status of the heating systems.

## 2 Current Drive Modelling

The physics of non-inductive current drive efficiencies is involved. For an accurate calculation of the ECH current drive efficiency  $\gamma_{\text{ECCD}}$ , parallel momentum conservation in the collision processes has to be ensured. The two momentum conserving codes (CQL-3D (Fokker-Planck) [2] and TRAVIS (adjoint technique) [3]) showed consistency in the benchmark. They yield a higher current drive efficiency (for typical ITER applications by  $\approx 20\%$ ) in comparison to the non-conserving approaches.

NBI can drive strong global current arising from the fact that due to  $Z_{\text{eff}} \neq 1$  and toroidal trapping, the electrons cannot perfectly shield the fast injected ion current. The calculation of the driven current requires the exact description of the ion birth profile due to ionisation and charge exchange and that of the slowing down process. For calculating the fast ion current, multi-step ionisation processes have to be taken into account [4], especially at high energy, necessitating an extension of the initially used cross-sections. Orbit effects are important to describe correctly the location of the driven current. It is therefore important that the magnetic equilibrium is accurately provided to account for the large orbits of the fast ions. The correct description of the electron shielding requires also precise equilibrium description to get the correct trapped electron fraction.

For the beam codes used and benchmarked in this study (OFMC [5] and NUBEAM [6]) differences of about 25% in the current drive efficiency appeared coming mainly from the fast ion current whereas the electron shielding agrees rather well. As the reason for the remaining discrepancies is presently not known both, NUBEAM and OFMC, were used in parallel and the discrepancies were considered as uncertainties. Power and momentum spreading by turbulent interaction with the background plasma are not considered.

Both ECH and NBI show similarly high  $\gamma$ -values in the core in the range of  $\leq 0.3$  ( $\text{A}10^{20}\text{m}^{-2}\text{W}^{-1}$ ; see Table 1). The radial dependence of  $\gamma$  depends on the trapped particle fraction increasing toward the plasma edge. Therefore,  $\gamma_{\text{NBCD}}$  stays fairly constant qualifying NBCD for global CD. Contrary to this,  $\gamma_{\text{ECCD}}$  drops sharply toward the edge, restricting low-field side ECCD to local current density profile control and control of MHD activity (neoclassical tearing mode and sawtooth instability). For MHD stabilisation, dedicated upper port launchers are installed in ITER [7].

ICH has modest current drive efficiency ( $\sim 0.08$  to  $0.15 \text{ A}10^{20}\text{m}^{-2}\text{W}^{-1}$  depending on the operating frequency).

## 3 Modelling results

The proposed heating mix was validated in reference [1] by varying the power ratios between the NBI, ECH and ICH systems. These results are summarized in the following two subsections.

### 3.1 Scenario-2

Operational Scenario-2 ( $I_p = 15$  MA,  $B_t = 5.3$  T,  $n_e = 10^{20}$  m<sup>-3</sup>) is based on strong core heating in order to access a good H-mode. Heating and CD during the current rise are needed to minimize flux consumption by achieving a low internal inductance  $li$  [8]. At  $li \approx 0.8$ , 30 Vs will remain for the plateau, which will allow 400 s burn phase. A bootstrap current fraction  $f_{bs} = I_{bs}/I_p \approx 0.2$  is expected.

For modelling, transport is taken from the theory-based GLF23 model [9], which reproduces experimental data well. It specifically reproduces the stiff temperature profiles as experimentally observed. In this case, the edge pedestal in the H-mode plays a dominant role because it governs the plasma temperatures over the whole plasma cross-section.  $Q > 10$  could only be achieved in a stable way with  $T_{ped} \geq 5.2$  keV, which could be the upper limit of realistically expected pedestal temperatures.

For ITER flat density profiles are assumed. There is, however, strong experimental evidence that depending on the dominant turbulence - a turbulent convective inward flow in the transport physics of Scenario-2 might peak the density profile toward low collisionality [10]. The GLF23 transport model predicts that the plasma density should get peaked in collisionless ITER plasmas. Because of the uncertainties of turbulent particle transport, in the simulations both flat and peaked density profiles were considered.

It is assumed in all simulations that transport between top of the edge barrier and the separatrix is reduced to the level which keeps normalised pressure gradient  $\alpha$  close to but below the critical level  $\alpha_{cr}$ .  $\alpha_{cr}$  was determined from the linear MHD stability codes MISHKA [11] and ELITE [12] corresponding to  $p_{ped} < 130$  kPa. The limit is indicated in Fig. 1 by the vertical line.  $T_e$  on top of the barrier is 4.6 keV. The width of the edge barrier  $\Delta = 6$  cm at the outer mid-plane was kept the same for all cases.

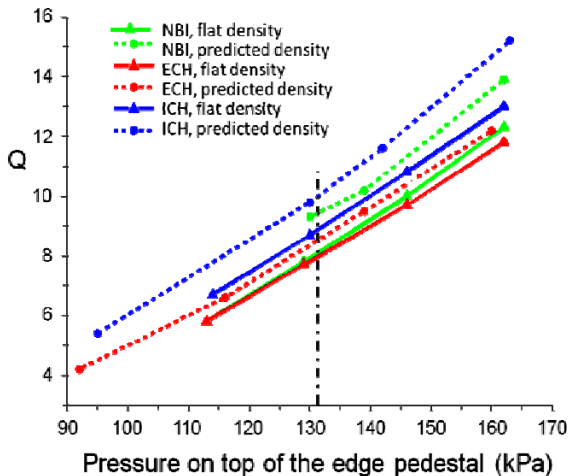


Figure 1. Fusion gain  $Q$  for 40 MW of either pure ICH heating (blue lines), pure NNBI with 1 MeV ions (green lines) and pure ECH (red lines) as function of thermal plasma pressure on top of the pedestal. Solid lines correspond to simulations with flat density profiles and dashed lines to peaked densities. The dashed-dotted vertical line is the expected edge pressure stability limit. 6 cm is taken for the barrier width.

The Scenario-2 plasma cases were simulated with JETTO [13]. Figure 1 summarises the main results of a generic plasma performance study addressing the specifics of the three heating methods and demonstrating the impact of the density profile. The absorbed power is 40 MW for each case, which is

the power level sustaining, along with the  $\alpha$ -particle heating, a  $Q = 10$  plasma. Peaked density profiles lead to a higher level of fusion gain  $Q$  than flat ones. There is a distinct difference in fusion gain between predominantly ion heating and pure electron heating with a  $\Delta Q$  of  $< 1.5$  between ICH and ECH. The difference in performance between the reference mix and pure electron heating amounts to  $\Delta Q_{max} < 1.0$ .  $Q$  is plotted in Fig. 1 against the edge pedestal pressure. With all reservations it is predicted that ITER will reach  $Q \approx 10$  marginally. But the proper choice of heating systems is of crucial importance. ITER has better chances to reach its  $Q = 10$  goal with peaked densities and those heating systems, which maximise ion heating (ICH). H-mode scenarios with improved bulk confinement, if accessible to ITER and not considered here, may ease access to  $Q = 10$ .

### 3.2 Scenario-4

Scenario-4 aims at large bootstrap and large externally driven currents. Because of the low current drive efficiencies of auxiliary systems current and density are reduced ( $I_p = 9$  MA;  $n_e = 0.7 \cdot 10^{20} \text{ m}^{-3}$ ). On the other hand, the plasma confinement time in tokamaks increases with  $I_p$  and density. In order to offset the performance reduced by the design parameters, plasmas with improved confinement ( $HH > 1$ ) have to be developed. This could be achieved with weak or reverse shear  $q$  profiles based on the empirical relation that more strongly reversed shear plasmas attain the larger HH factors. Possibly assisted by strong plasma flow a transport barrier develops inside the  $q$ -minimum, which - together with the one caused by the H-mode edge pedestal ( $\Delta f_{bs}^{edge} \approx 20\%$ ) - provides the needed level of bootstrap current.

These maximum performance plasmas of Scenario-4 [14] have large  $\beta_N$  and reside near the operational and stability limits. The stability depends on the pressure peaking factor and the current density profile and has to be improved by additional external measures e.g. to cope with resistive wall modes. As a consequence, there is a strong link between pressure and current density profiles. As the bootstrap current is generally much larger than the externally driven current the major goal of a heating method is to serve as actuator providing access to plasmas with good confinement and a high  $f_{bs}$ .

Heating Scenario	ECCD				NBCD			ICH	global	
	P (MW)	$\gamma_{CD}(0)$	$\gamma_{CD}(0.4)$	$I_{CD}$ (MA)	P (MW)	$\gamma_{CD}$	$I_{CD}$ (MA)	P (MW)	$\langle \gamma_{CD} \rangle$	$f_{CD}$
<b>A</b> /20/33/20	20		0.16	0.7	33	0.3	2.3	20	0.25	0.34
<b>B</b> /53/0/20	53	0.22	0.16	2.4	0		0	20	0.2	0.27
<b>C</b> /73/0/0	73	0.22	0.16	3.4	0		0	0	0.2	0.38
<b>D</b> /40/33/0	40	0.22	0.16	1.7	33	0.3	2.3	0	0.23	0.45

Table 1: CD efficiencies  $\gamma [10^{20} \text{ m}^{-2} \text{ AW}^{-1}]$ , driven currents  $I_{CD}$ , the assumed global CD efficiency  $\langle \gamma \rangle$ , and the global current drive fraction  $f_{CD}$  for the heating scenarios A-D for ITER Scenario-4.

Unlike Scenario-2, where the CD characteristics of the heating methods do not critically enter, Scenario-4 was analysed with the help of four distinctly different heating mixes. Heating scenario A represents the baseline ITER mix. All considered cases A-D sum up to 73 MW absorbed power. Table 1 lists the power mix and the current drive signatures of each case.

Figure 2 shows the relation between  $Q$  and the non-inductive current fraction  $f_{ni} = f_{bs} + I_{CD}/I_p$  with the assumption  $f_{bs} = 0.5$  for  $P_{ICH} = 0$  (C, D; solid curves) and  $P_{ICH} = 20$  MW (A, B; dashed curves). The four reference cases A-D are plotted as solid points; also variants of A and C were studied. These cases are results of steady state solutions of iterative 1-D transport modeling using GLF23 transport model together with existing DIII-D boundary information [15].

High  $Q$  values are obtained with NBI or ECH, respectively. But only the scenarios with NBCD reach  $f_{ni}$  values above 0.8. Direct ion heating provides case B with a higher  $Q$  than case C. Detailed simulations around the heating scenarios A and C were carried out. Using NBI and ECRH/ICH in various combinations, which always add up to 73 MW, high  $f_{ni}$  and  $Q$  ( $f_{ni} \approx 0.8-0.9$ ,  $Q \approx 4.5-5$ ) can be obtained. With ECCD alone, tests have been made using the technical ECCD injection flexibility foreseen at ITER.  $f_{ni}$  drops typically below 0.7 and about 2MA are missing, even increasing the ECCD efficiency by 30%. It is obvious that only with NBCD and optimised scenarios can one reach  $f_{ni}$  values near 0.9 and  $Q$  near 5.

The studies presented here are indicative and not yet fully optimized. Better  $Q$  values might be obtained with lower power e.g.  $P_{ECCD} = 53$  MW instead of 73 MW for the steady-state phase.

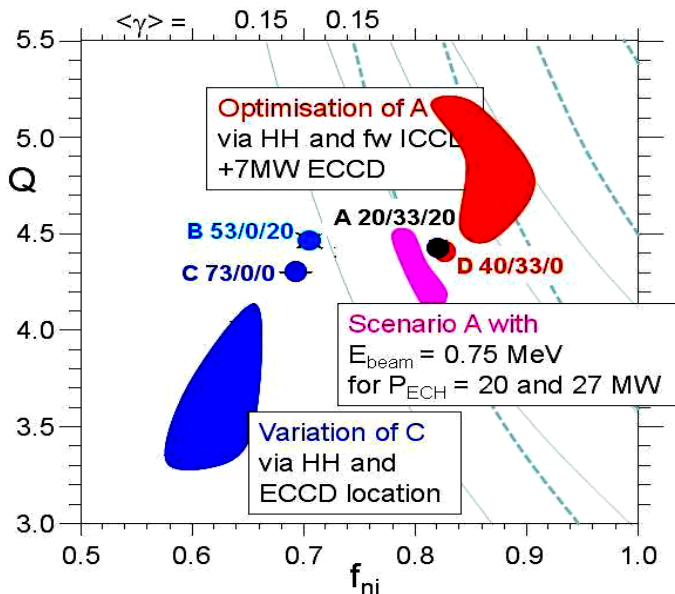


Figure 2. Operational space of  $Q$  versus the non-inductive current fraction  $f_{ni}$ . Shown are the cases A-D and variants of A and C. For mix A, the consequences of reducing the beam energy to 0.75 MeV was also investigated. The curves are based on the simple relation with  $f_{bs} = 0.5$  and variable  $\langle \gamma \rangle$ . The solid curves are with  $P_{ICH} = 20$  MW, the dashed ones with  $P_{ICH} = 0$ .  $\langle \gamma \rangle$  starts with 0.15 and increases in steps of 0.05 up to 0.3 for the 2 cases.

Facing the difficulty with reaching truly steady-state conditions, it is worthwhile to also assess heating scenarios with  $f_{ni} < 1$ , which maintain a small inductive current of the order of 1 MA [16]. The ITER baseline heating scenario A has been studied with the GLF23 model and the fast transport code

(FastTran), ONETWO and EFIT [17]. These runs have been performed keeping the total plasma current fixed at 9 MA. With an off-axis NBCD set-up, a reduction of  $f_{bs}$  by 0.1 compensated by an ohmic contribution of  $\approx 1$  MA,  $Q \approx 4.5$  can be achieved. These discharges with finite ohmic current will allow ITER to reach the pulse length goal and they will play an important role in the development of steady-state scenarios and the preparation of the steady-state technology.

The following special cases were modelled mostly in the spirit of sensitivity studies:

**High edge pedestal temperature:** With the assumption of a high edge pedestal ( $T_{ped} > 7$ keV) leading to a high edge bootstrap current contribution, stationarity is obtained with the non-inductive fraction,  $f_{ni}$ , even in excess of 100%;  $f_{bs} = 0.7$ ,  $Q = 5.3$ , and  $\beta_N = 3.1$  [18].

**High internal transport barrier:** In this case weakly or strongly reversed  $q$ -profiles have to be tailored and sustained.  $q(\rho)$  and  $\chi(\rho)$  profile need to be consistent. It has been verified that there is the technical flexibility at ITER to correspondingly shape the  $q$ -profile by ECCD. With the improved equatorial launcher (EL) having one row in counter-CD, the necessary  $q$  profiles – zero shear, weakly and strongly reversed shear - can be produced and controlled under conditions close to the ITER reference scenarios [19].

In a sensitivity study a weak shear case was explored in detail with 50 MW of NBI and 20 MW of ECCD. HH was assumed to be 1.37.  $f_{bs} \approx 0.5$  without a high temperature pedestal. At  $I_p = 8.5$ MA  $Q = 5$  was achieved steady state.

**Case with ECCD alone:** ECCD with  $P_{CD} = 50$  MW and 70 MW was studied. Without NBCD, the total current drops to 6 MA causing a serious reduction in performance. 50 MW ECCD yield  $Q \approx 3$  with HH = 1.37 [20]. One way of compensation is by increasing the HH factor (and scaling thereby the effective  $\chi(\rho)$ ). Again in the spirit of a sensitivity study HH has been varied between 1.3 and 1.78. Even for the highest HH factor the performance losses due to the lower total plasma current are not recovered. No steady-state scenarios are found with  $f_{ni} > 0.85$  and  $Q$  near 5 with ECCD only or with ECCD and ICCD.

**Cases with Lower Hybrid CD:** Steady-state profiles have been obtained with weak and strongly reversed shear with 33 MW of NBI and 34 MW of LHCD at an HH factor of 1.37.  $Q = 5$  at  $I_p = 9$  MA is achieved with profiles similar to the ITER reference ones.

For an RF-only case (LHH, ICH, ECH) [21] current density maxima of  $j_{bs}$  and  $j_{ECCD}$  coincide at  $\rho = 0.45$ . Here an ITB develops, which is triggered and locked by ECCD. The LHCD power deposition is located at  $\rho = 0.7$  and the current drive obtained ( $\approx 0.6$  MA) contributes to the total

non-inductive current fraction ( $f_{ni} \approx 0.97$ ). ICH provides central heating. Currents driven inside the ITB have been found to lead to shrinking and final collapse of the ITB itself [22]. The details depend, however, on the transport model relating shear and  $\chi$ . With this current drive scheme, the  $q$  profile obtained is stable for 1000 s at  $I_p = 8$  MA, with  $q_0 \approx 6$  and  $q_{min} > 2$ ,  $Q = 6.5$  is obtained. This scenario is, however, rather demanding in terms of MHD. A way to overcome the MHD problems is cyclic operation as suggested in [23].

Considering the substantial effort required a critical issue is whether NNBI can also drive the current of DEMO. DEMO can be heated without NBI and steady state current drive can be achieved with ECCD. However, the increased CD power required in this case necessitates an enlargement of the unit size to deliver the same output. This leads to an increase of perhaps 25% both in the capital and the electricity costs, the cost driving factor being the recirculating power for CD [24]. Whereas a steady state DEMO with NBI needs a CD power of about 200 MW, it will need twice that power with ECCD. Though, for ITER, the beam voltage can be reduced to 0.85 MeV (at higher current density to maintain the specified power) the R&D for the NBI system should, however, remain targeted for 1 MeV beam energy, which will – considering also DEMO - reduce the overall development costs.

#### 4 Technical development of the heating and current drive systems

The maturity of the H&CD technologies has an important factor on achieving the ITER goals. The H&CD systems required for ITER are an extensions of the power densities, pulse lengths and power unit source for the NB, EC, IC and LH systems relative to the present day technology. R&D efforts on all systems are underway to reduce technical and schedule risks associated with the installation of these systems at ITER.

##### 4.1 NBI

In order to obtain the high performance beams required for ITER stably and reliably, several issues need to be solved. These include uniform illumination of the entire accelerator aperture array ( $\leq \pm 10\%$ ) with  $D^-$  or  $H^-$  in order to produce low divergence beamlets from the entire array, reliable source start-up, reliable source operation at  $\leq 0.3$  Pa in order to reduce the stripping losses and power loading of the accelerator grids to acceptable levels, temperature control of the plasma grid, low co-extracted electron currents, and stable high voltage holding. To attain the specified beam performance, many R&D and design activities are underway on these tasks. In parallel, construction has started of the Neutral Beam Test Facility (NBTF), which includes MITICA, which is essentially a full size, full power and pulse length NNBI, and SPIDER, which is a full ITER size, full power, and full pulse length ion source test bed. SPIDER will be used to carry out the final development of the ITER ion source, whilst MITICA will finalise the development of the 1 MV accelerator, carry out integrated testing of the NNBI, demonstrate the beam performance required in ITER and develop all the conditioning and commissioning protocols and procedures for the ITER NNBI.

Further developing negative neutral beam technologies could significantly improve reliability and efficiency for possible application on DEMO. This includes Cs-free operation, electrostatic residual ion dump studies, space charge neutralisation, physics of extraction of negative ions, alternative neutraliser technology and assessment of their potentiality as off-axis current drive source.

##### 4.2 ECH

The EC system is comprised mainly of four parts: high voltage power supplies (HVPS), gyrotrons, transmission lines (TL) and launchers. The technological challenges facing the EC system rest primarily with the gyrotron and launcher development. The gyrotrons are to be procured by four domestic agencies (EU, IN, JA and RF). Japan has produced a 170 GHz 1 MW prototype tube that has demonstrated  $> 800$  s operation and Russia has also demonstrated 1 MW operation but short

pulse lengths of  $> 200$  s (limited by the power supply). Europe is embarking on a 2 MW coaxial gyrotron development and multiple prototypes that have a stepwise increase in pulse length. The first prototype has demonstrated  $>1.6$  MW and 15 ms operation, and is now being revised and expected to be tested for  $\geq 2$  MW  $>2$  s operation in 2010. The India gyrotron will either rely on one of the other domestic agencies or their own growing gyrotron development program. Note that the first gyrotron delivery is scheduled for 2016, offering  $> 4$  years of prototype testing and development for increased reliability and functional capabilities before proceeding with the series production for ITER.

Two launcher types are envisioned for ITER: one equatorial for central H&CD applications and four upper port launchers for control of MHD activities. The launchers divide the power injection into sets of 4 to 8 MW, which is a four to eight fold increase over present day launcher handling capabilities. In addition the launchers will be for CW operation and subject to nuclear heating. Prototype and high power testing of launcher components and mock ups are envisioned to ensure reliable operation compliant with the ITER parameters.

### 4.3 ICH

The IC system is also comprised of four main subsystems: power supplies, sources, transmission line and antenna. The technology for the power supplies and transmission line is compatible with existing industrial technology, while the sources and antenna require further development. The sources are to provide 5 to 6 MW (VSWR of 1.2 to 1.5) over a frequency range of 40 to 55 MHz, which is an increase in output power per source relative to existing IC systems. The antenna represents the greatest challenge for the ITER IC system. The antenna has to ensure high coupling in a variety of plasma scenarios and edge densities. Results from the JET ITER-like antenna have provided valuable experience for further developing the final ITER antenna design. In addition, a second antenna has been accepted into the baseline, which allows decreasing the voltage applied on the antenna and provides more operational safety and a greater flexibility in plasma coupling without compromising the power.

### 4.4 LH

A LH system with up to 40MW is included in the ITER baseline design, albeit not as part of the initial construction phase [25]. The development is being advanced by an international partnership on a voluntary basis. The main challenges are associated with the source development and window design for the confinement barrier. The source is envisioned to operate at 5 GHz and provide an output power of 0.5 MW, which is equivalent to the sources being developed for KSTAR. The existing 3.7 GHz, 0.5 MW sources offers an alternative in the event the KSTAR sources development encounters setbacks. The in-line windows form a confinement barrier that prevents the propagation of tritium and other contaminants up the waveguide. The present technology for in-line windows uses Boron Oxide, which are brazed into the waveguide. High electric fields are generated locally at the window - brazing - waveguide interface, which may result in internal breakdown followed by failure of the window. Alternative designs using CVD diamond windows are being explored. Note that the installation of the LH system is not envisioned until after 2023, which provides additional time for further development and prototype testing.

## 5 Conclusions and summary

In summary, a proper mix of heating and CD systems provides the necessary actuators to respond in a flexible way for the development of the best possible ITER scenarios: ICH offers flexibility in scenarios and may provide the final increment to the  $Q = 10$ -goal; ECH is technically mature and allows to shape the current density profile in a unique way. Its off-axis CD efficiency is too low, however, to serve as exclusive current drive method. NBI seems to be indispensable due to the high current drive efficiency. In addition, it can be flexibly used at different B and  $I_p$  values during

scenario development. The technical development risks with beam energies up to 1 MeV are high, however. A lower beam energy target of 0.85 MeV would be acceptable for ITER. For the DEMO needs the NNBI R&D should, however, target for 1 MeV beams.

Only ITER can demonstrate the self-organised plasma characteristics with strong central self-heating by fusion  $\alpha$ -particles. The presently foreseen heating mix seems to best ensure the accessibility to the full range of ITER operation scenarios whilst providing the flexibility required for an experimental device. The heating mix seems to be uncritical for Scenario-2 and could be NBI, ICH as well as ECH. ICH and a peaked density profile would support the development of  $Q = 10$ . H-mode versions with improved core confinement – not considered in this study – could overcome possible limitations of the baseline scenario. For safely accessing the H-mode (and in case full power specification is not reached in all system cases) an increase of the ECH power by additional 20 MW should be considered.

Scenario-4 clearly needs in-situ development and will be part of the experimental programme of ITER. For its success, a flexible heating system is necessary. Secondary characteristics of the various methods can be utilised as actuators to induce specific plasma responses. Owing to the limitations in the CD efficiencies of the presently foreseen systems, LH is maintained in the baseline for use at a later experimental stage.

*The views and opinions expressed herein do not necessarily reflect those of the ITER Organization*

## References

- 
- [1] F. Wagner et al., to be published in Plasma Phys. Contr. Fusion
  - [2] R. W. Harvey and M. G. McCoy, in Proc. IAEA Tech. Comm. Meeting 1992 (IAEA, Vienna, 1993), p. 498.
  - [3] N. Marushchenko et al., Nucl. Fusion **48** (2008) 054002.  
N. Marushchenko et al., Nucl. Fusion **49** (2009) 129801.
  - [4] T. Oikawa et al., Nucl. Fusion **41** (2001) 1575.
  - [5] M. Tuszewski and J.P. Roubin, Nucl. Fusion **28** (1988) 499.
  - [6] A. Pankin et al., Comput. Phys. Commun. **43** (1981) 61.
  - [7] G. Ramponi et al., Fusion Engin. Design **82** (2007) 454.
  - [8] A.C.Sips et al., 22<sup>nd</sup> IAEA Fusion Energy Conf., paper IAEA-CN-165/IT/2-2
  - [9] R.W. Waltz, *et al.*, Phys. Plasmas **4** (1997) 2482.; and <http://w3.pppl.gov/NTCC/GLF>
  - [10] C. Angioni et al., Phys. Rev. Lett. **90** (2003) 205003.
  - [11] A. B. Mikhailovskii et al., Plasma Phys. Rep **23** (1997).
  - [12] P. B. Snyder et al., Phys. Plasmas **9** (2002) 2037.
  - [13] G. Cenacchi and A. Taroni, in Proc. 8th Comput. Physics, Computing in Plasma Physics, Eibsee, 1986; European Physical Society, Petit-Lancy, 1986, Vol. 10D, p. 57.
  - [14] Progress in the ITER Physics Basis, Nucl. Fusion **47** (2007) S285.
  - [15] J.M. Park et al., 3<sup>rd</sup> ITPA IOS TG meeting (Frascati, 2009) to be submitted to Nucl. Fusion.
  - [16] R. V. Budny, Phys. of Plasmas **17** (2010) 042506.
  - [17] H. St. John et al., in Proc. Conf. Contr. Fusion and Pl. Phys., Lisboa, 1993 (Europ. Phys. Soc, Geneva, 1993) Vol. I, p.99.
  - [18] G. Giruzzi *et al.*, 21st IAEA Fus. Energy Conf. (2008), paper IT/P6-4.
  - [19] C. Zucca, 2009 *PhD Thesis* EPFL, no 4360 <http://library.epfl.ch/en/theses/?nr=4360>.
  - [20] O. Sauter and C. Zucca, *On the Role of Heating and Current Drive Sources on the Scenario 4 for ITER: preliminary results with EC only* (June 2009), report.
  - [21] J. Garcia *et al.*, Phys. Rev. Lett. **100** (2008) 255004.
  - [22] P.T. Bonoli *et al* 2006 *Proc. 21st Int. Conf. on Fusion Energy 2006 (Chengdu, China, 2006)* (Vienna: IAEA) CD-ROM file IT/P1-2.
  - [23] J. Garcia et al., Nucl. Fusion **50** (2010) 025025
  - [24] D. Ward, to be published in Plasma Phys. Contr. Fusion.
  - [25] G.T. Hoang et al., Nucl. Fusion **49** (2009) 075001.